PCCP

A physical mechanism for large-ion selectivity of ion channels

Dirk Gillespie,[a] Wolfgang Nonner,[a] Douglas Henderson[b] and Robert S. Eisenberg[c]

[a] *Department of Physiology and Biophysics, University of Miami School of Medicine, P. O. Box 016430, Miami, FL 33101, USA. E-mail: dirkg@chroma.med.miami.edu; wnonner@chroma.med.miami.edu*

[b] *Department of Chemistry and Biochemistry, Brigham Young University, Provo, UT 86402-5700, USA. E-mail: doug@huey.byu.edu*

[c] *Department of Molecular Biophysics and Physiology, Rush Medical College, 1750 W. Harrison St. #1291, Chicago, IL 60612, USA. E-mail: beisenbe@rush.edu*

Received 2nd April 2002, Accepted 5th August 2002
First published as an Advance Article on the web 30th August 2002

Many biological ion channels preferentially conduct large ions over small ions. Here we propose a simple mechanism for this large-particle selectivity. Size selectivity is examined using a hard-sphere model of a binary fluid in a two-compartment system that represents a bath and the selective section of a channel (filter). The solvent is assigned a small repulsive excess chemical potential in the filter. Under these conditions, larger solutes are absorbed into the filter in greater numbers than small solutes because of a negative pressure difference between the filter and the bath. To model the selectivity of ion channels, we extend the model to a hard-sphere electrolyte and a filter that contains, in addition to particles exchanged with the bath, structural ions that are confined to the filter and introduce charge selectivity. This system also selects for the larger ions. For this system, the pressure in the filter varies greatly as a function of bath concentration. Because this would result in large forces acting on the channel protein, we also consider a constant-pressure system and allow the volume to vary. In that case, we observe ion concentration-dependent increases in filter volume and ion density that result in conductance properties observed in some channels.

I. Introduction

Biological ion channels, in general, perform two functions: they open (gate) and, when open, they selectively conduct ions across a membrane.[1] The degree of selectivity of each channel type has evolved to meet the needs of the channel's function. Some channels are only weakly selective for cations or anions (for example, the ClC anion channel family[2] and cation channels like the nicotinic acetylcholine receptor and gramicidin A[1]). Other channels are highly selective for one physiological ion (for example, the L-type calcium channel, the voltage-gated sodium channel, and the potassium channel[1]). Here we study channels that preferentially conduct larger ions over smaller ones.

On the face of it, a preference for large ions is counterintuitive in a molecular channel; why would a large ion partition into an apparently entropically unfavorable small space like a channel? Recently, Goulding *et al.* have shown how large-particle selectivity can arise in hard-sphere fluids that are confined in small geometries.[3,4] Considering spherical cavities, cylindrical pores, and slit geometries, they found that changing the ratio of solvent diameter to geometric spacing (specifically, diameter of the sphere or cylinder and spacing of the confining slit walls) produces ranges of small-particle selectivity and ranges of large-particle selectivity.

In this paper we extend the concept of entropic size selectivity developed by Goulding *et al.* to systems that do not have hard walls, but include a solvent–channel interaction. By considering an uncharged system of two hard-sphere fluids in equilibrium (one of which represents the ion channel), we find that substantial large-particle selectivity can arise *via* excluded-volume effects if the solvent–channel interaction creates a small energetic penalty for solvent entering the channel. Next, we model several kinds of ion channels by applying the same model to ionic solutions with simple representations of the channels' selectivity filters. We find that the same excluded-volume mechanism produces many selectivity effects exhibited by anion channels, as well as cation channels like the acetylcholine receptor and gramicidin A. More generally, this mechanism might be important for the large-ion selectivity seen in many ion/protein interactions.

II. Theory

We break our analysis in two pieces: first we consider only hard-sphere fluids to show how size selectivity arises and then we include ions into the calculations.

First, we consider two compartments of hard-sphere fluids in equilibrium, the "bath" with known concentrations and the "filter" (the selectivity filter of the channel) with particle concentrations to be determined. The filter contains a given concentration of confined particles; these model the amino acid residues of the channel protein that are tethered to the wall of the channel and behave much like free particles within the filter. These structural particles introduce an asymmetry of particle densities between the bath and the filter, and selectivity is determined by the balancing of excluded volume forces, in our case calculated with Percus–Yevick theory.[5] The numerical implementation of this situation is the same as previously described for charged hard-sphere fluids with the electrostatic components removed.[6,7] An overview of the theory is given in the appendix.

Whereas in the mechanism described by Goulding *et al.* the well-defined (hard, smooth wall) geometry of the pore is crucial, it is important to note that in the mechanism we propose

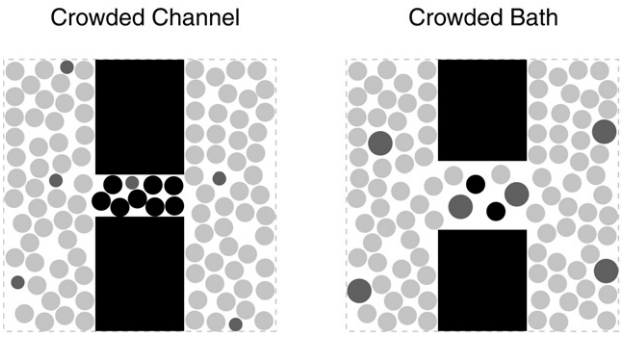

Fig. 1 Schematic diagrams of the two types of channels. The spheres represent the solvent (light grey), solute (dark grey), and groups confined to the filter (black). Black: membrane and protein. Note that density differences are exaggerated for the sake of illustration (see Fig. 2c).

here a precise geometry is not necessary for selectivity to occur. We emphasize this fact in our analysis by describing the bath and the filter solutions as bulk fluids. In this view, packing effects in the filter are not constrained by the filter wall but rather are described as continuing over some radial distance into the atom layers of the pore wall (for a more detailed discussion, see refs. 7 and 8). Thus our "filter volume" is analogous to a sample volume of an unbounded bulk fluid.

We consider two basic cases: the *crowded filter* with a high concentration of structural particles (53.1 M which corresponds to 8 particles in 0.25 nm^3) and the *crowded bath* (that is, crowded relative to the filter) with a low concentration of structural particles in the filter (4.4 M which corresponds to 2 particles in 0.75 nm^3). This is illustrated in Fig. 1. For each case, the two compartments are equilibrated given 55.5 M of the 0.28 nm-diameter solvent (the solvent primitive model, SPM, of water) and 0.1 M of the solute in the bath. The results for each case are shown in the curves without asterisks in Fig. 2a where the partitioning coefficient for the solute (the ratio of filter concentration to bath concentration) is plotted as a function of solute diameter. In both cases only small-particle selectivity is observed. To produce large-particle selectivity, we introduce a small penalty for solvent entry into the filter. The results of adding a $1kT$ penalty for the solvent are shown in the curves with asterisks in Fig. 2a. For the crowded filter, there is little change in selectivity, but for the crowded bath the situation has qualitatively changed; now, partitioning *increases* as a function of solute diameter.

The reason for large-particle selectivity is illustrated in Fig. 2b where the difference in filter and bath pressures is shown for the four simulations of Fig. 2a. Comparing the results of the crowded filter (dashed) curves with and without the solvent penalty, it is clear that the result of the solvent penalty is to lower the pressure in the filter. In the crowded filter case there is little effect on size selectivity because in both cases the pressure in the filter is always greater than in the bath, forcing particles out of the filter, with larger particles being driven out more.

In the crowded bath case, the structural particles are at a much lower concentration and there are fewer excluded-volume interactions; the solute concentration in the filter is approximately that of the bath (Fig. 2a) and the filter/bath pressure difference is approximately zero (Fig. 2b) when there is no solvent penalty (solid curve without asterisk). However, when a solvent penalty is imposed on the water in the filter, the filter pressure is lower than the bath pressure (solid curve with asterisk in Fig. 2b), forcing particles *out* of the bath and *into* the filter. With larger particles being driven out more, they accumulate in the filter, resulting in the opposite selectivity of the crowded filter case. This selectivity requires that the filter maintains its volume under a negative pressure so that the channel does not collapse.

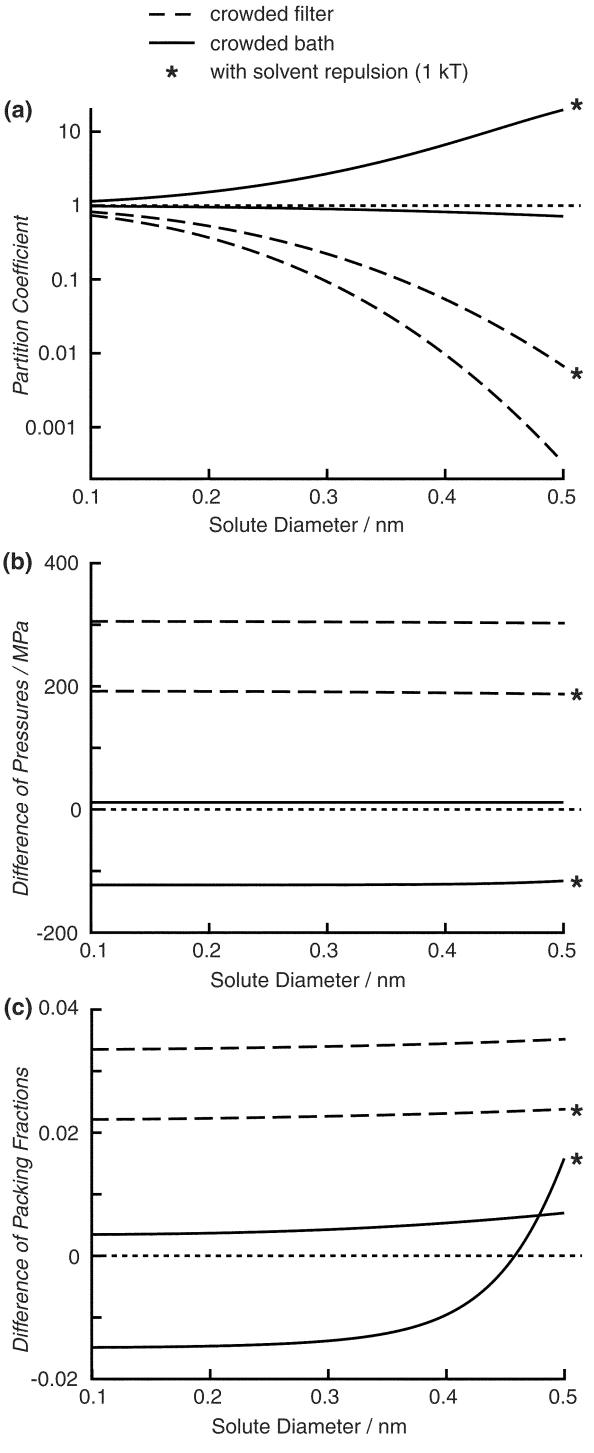

Fig. 2 Selectivity for an uncharged solute. The two systems of Fig. 1 are considered: the crowded filter (containing 8 confined particles of 0.28 nm diameter in a volume of 0.25 nm^3, dashed curves) and crowded bath (filter containing 2 confined particles in 0.75 nm^3, solid lines). The bath contains a two-component fluid of hard spheres. (a) filter/bath partition coefficient of the solute *versus* solute diameter; (b) (bulk) pressure of filter relative to bath; (c) difference in packing fractions between filter and bath. The curves marked by an asterisk (*) involve $1kT$ of penalty to solvent in the filter.

An alternate, but more heuristic, explanation of large-particle selectivity is to consider the difference in filter and bath packing fractions, as shown in Fig. 2c for the four simulations of Fig. 2a The packing fraction

$$\eta = \frac{\pi}{6}\sum_i \rho_i \sigma_i^3 \qquad (2.1)$$

is the fraction of space occupied by all the different particle species i with diameter σ_i and number density ρ_i, and thus the difference in packing fraction between the two compartments is a heuristic measure of how particles wish to partition; the smaller the packing fraction in the filter (as compared to the bath), the more favorable entry of another particle is. (However, since the packing fraction does not exclusively determine the chemical potential of this binary system, this argument breaks down at large solute diameters, as shown in the change of sign for the solid curve with an asterisk in Fig. 2c.)

The solvent penalty lowers the packing fraction in the filter. As with the pressure differences, this reduction in packing fraction is only significant when the filter has low structural particle concentration and is thus not a priori more space-filled than the bath. Only then can the reduction in filter packing fraction result in a filter packing fraction that is less than the bath packing fraction, making the filter entropically more favorable than the bath, especially for large particles. This effect is greatly exaggerated in Fig. 1.

In passing we note that, although the penalized and nonpenalized solvent cases have quite different macroscopic outputs, the differences in packing fraction in the two cases are quite small (less than 5% of the bath packing fraction). Such a small difference might be difficult to detect in structural studies of protein cavities because the difference in packing fraction is translated into a distance by a cube-root law.

A Sources of solvent penalty

So far we have only described the addition of a penalty for the solvent to enter the filter. We now consider how such a penalty may arise in ion channels. One kind of penalty is geometric; the solvent's size makes it difficult to enter and pack in the filter, a case considered by Goulding, *et al.*[3,4] A more general kind of penalty can orginate from any physical aspects of the channel that involves surface work in creating the water/protein interface. This was observed in molecular dynamics of SPC/E water in a bulk solution/slit/bulk solution configuration where a reduction of water density in the slit occured when the attractive component of a Lennard-Jones potential between the water and slit wall was removed.[9] (The effective 0.9 nm width of the slit used in this calculation is comparable to the size of the cavities that we envision.) In channels apolar amino acid residues (such as those in the selectivity filter of ClC channels[2]) can have the same effect. Our model does not explicitly include such surface effects; thus we parameterize this small, but essential penalty as an excess chemical potential for filter water.

It is possible to estimate an upper limit for this penalty by considering the surface work for a water/air interface, for example the interface of a cylindrical pore of length 1 nm and radius 0.5 nm. This has a surface area of 0.314 nm^2, corresponding to a surface work of $55.5kT$ given 7.2×10^{-2} J m^{-2} for the surface tension of water. The cylinder volume holds approximately 26 water molecules, and thus, on average, each water molecule contributes approximately $2.1kT$ to the surface work. The ion channels we consider have cross-sections[1] that ensure that the large majority of water molecules in the channel participate in the surface formed with the protein. Thus, it is reasonable to assume uniform energetic penalties for all water molecules; in wider cavities or planar surfaces, partitioning effects as described here will be restricted to the solution layer next to the protein.

Another estimate is applicable when the solvent does not wet the filter (that is, when the water must evaporate into the filter). In that case, one can estimate the penalty per water molecule by the Gibbs free energy of evaporation, which is 8.7×10^3 J mol^{-1} at 25 °C. This corresponds to $3.5kT$ per water molecule.

B Combining electrostatics and the crowded bath

In order to apply the proposed principle of large-particle selectivity to ion channels, we now include ions in the baths as charged hard spheres, typically Na^+ and Cl^- of diameter 0.2 and 0.362 nm, respectively, in 55.5 M of SPM water. In the filter, the structural particles are given charge to simulate the charges of the protein that are exposed to the selectivity filter. We assign partial charges to the confined particles, in agreement with new structural studies on ClC anion channels.[2] The structural charge in the model attracts ions to the filter and provides charge selectivity. In equilibrating the bath and filter, the calculation methods are the same as previously described (see refs. 6 and 7 and the appendix) with the excess chemical potentials calculated with the mean spherical approximation (MSA).[10–12] In the electrostatic calculations, a uniform permittivity of 78.5 is used for both for the bath and the filter.

Because we treat both bath and filter as bulk fluids, the filter is necessarily charge-neutral. Our computations thus are likely to overestimate counterion concentrations that would occur in the small geometry of real channels, particularly when ion concentrations in the bath are small. If real channels are *less* crowded with counterions than our bulk solutions, they will be even more selective than our model. The selective effects we observe then should represent lower limits.

Selectivity among anions has previously been associated with reduced permittivity in the filter of CFTR anion channels. Following Born's treatment of hydration, Smith *et al.*[13] concluded that such a filter repels large ions less than small ions. An unspecified force was postulated to provide generic attraction for anions. If structural charges were explicitly included in such a model, the electrostatic ion–ion interactions in the filter (which become stronger in a weak dielectric) would tend to compensate for the energetic cost of moving ions from bulk water into a weak dielectric. A case of structural charge in a weak dielectric has been studied by Nonner *et al.* for calcium channels;[7] the net electrostatic effect in these computations was that small ions are attracted over large ions.

III. Anion channels

A Ion accumulation

To model the filter of an anion channel, we include three structural ions with $+1/2$ charge and 0.3 nm diameter and two structural ions with $-1/2$ charge and 0.28 diameter nm, giving the filter an overall $+1/2$ structural charge to attract anions. To understand the importance of various parameters, we consider two different filter volumes (0.375 and 0.75 nm^3) bathed in NaCl solutions from 10 mM to 1 M. In both filters, a $1kT$ penalty for water partitioning into the filter produces large-ion selectivity. In Fig. 3a we show how the number of accumulated anions and cations changes as a function of bath concentration. In both cases, in the physiological concentration range from 10 to 100 mM, the filters accumulate only Cl^-, but at higher concentrations the small and large filters accumulate ions differently, with the large filter accumulating more ions (both Cl^- and Na^+) than the small filter. This effect is thought to occur in several types of anion channels where, at high bath concentrations, the Na^+ current can become comparable in size to the Cl^- current while at low bath concentrations the total current is the Cl^- current.[1,14]

One part of the attraction of the anions to the filter is the long-range electrostatic potential difference between the filter and the bath (the Donnan potential) shown in Fig. 3b. The Donnan potential is positive at low concentrations for both filters and changes by approximately 80 mV over the range of bath concentrations shown, even becoming negative for the

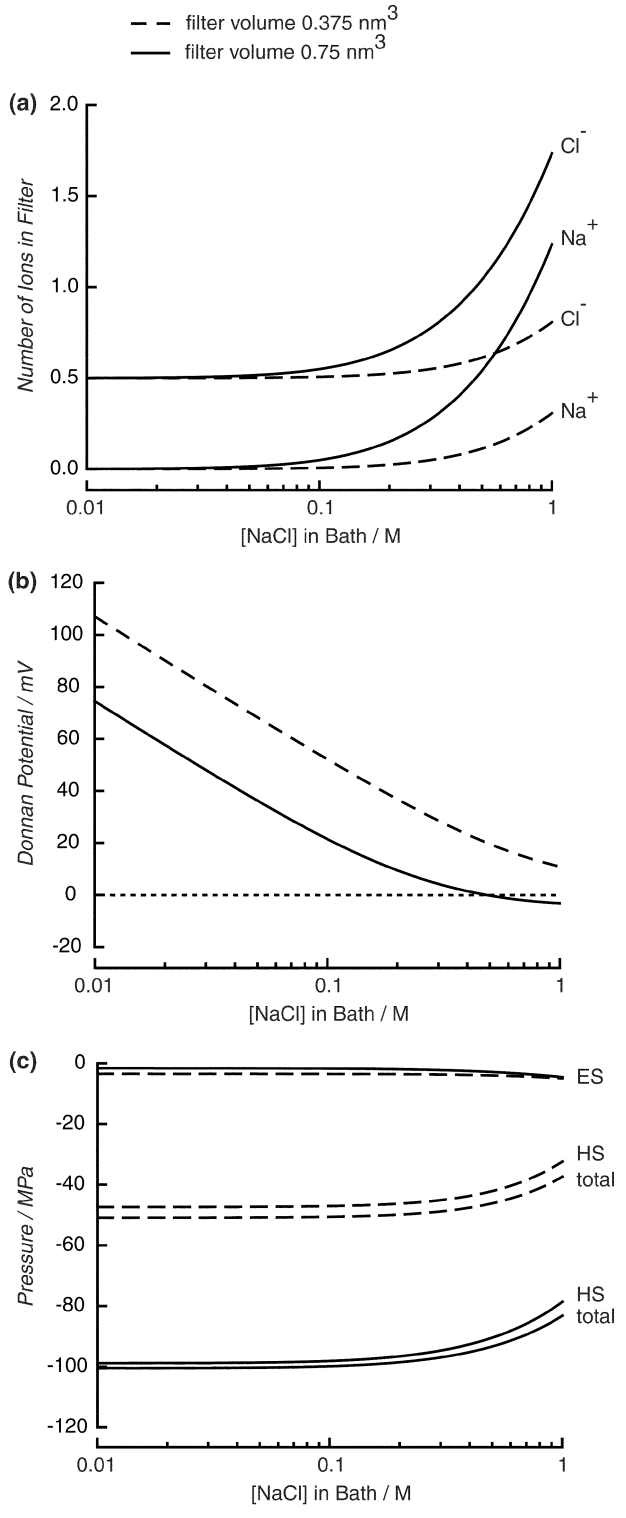

Fig. 3 Characteristics of two model anion channel (crowded-bath) systems. The filter confines 3 particles of charge $+1/2$, diameter 0.3 nm, and 2 particles of charge $-1/2$, diameter 0.28 nm, in volumes of either 0.375 or 0.75 nm^3. The bath contains a model electrolyte solution (55.5 M SPM water and varied concentration of charged hard spheres representing Na^+ and Cl^-). (a) Numbers of Na^+ and Cl^- in the filter *versus* NaCl concentration in the bath; (b) electrostatic potential of the filter relative to the bath; (c) pressure in the filter with respect to the bath and its electrostatic (ES) and excluded-volume and ideal (HS) components. Note that the electrostatic contribution is very small; the hard-sphere pressure dominates.

large filter at high bath concentrations. This behavior of the long-range electrostatic potential underlies the variation in anion/cation selectivities.

Lastly, Fig. 3c shows the pressures inside the filters. Both the hard-sphere and electrostatic components of the pressure in the filter are negative with respect to the bath, but the (local) electrostatic component of the pressure is insignificant. (This component would be selective for small ions over large ions.[6,7]) Thus the partitioning of ions into the filter from the bath is due almost exclusively to excluded-volume (hard-sphere) effects and long-range Coulombic force.

B Large-ion selectivity sequence

Anion channels preferentially select larger anions over smaller ones.[1,15,16] As discussed above and shown in Fig. 2b, in our model this is a result of excluded-volume effects, with the larger ions having more entropic force acting on them. For the model anion channels discussed above, Fig. 4 shows the quantitative results of selectivity as a function of monovalent anion diameter.

Fig. 4a plots the partition coefficient between the bath and the filter *excluding* the effect of the Donnan potential. Specifically, the chemical potential of species i is given by (see ref. 7 and appendix)

$$\mu_i = kT\ln(\rho_i) + ez_i\Psi + \mu_i^{\mathrm{ex}} = \mu_{\mathrm{B},i} = kT\ln(\rho_{B,i}) + \mu_{\mathrm{B},i}^{\mathrm{ex}} \quad (3.1)$$

where the subscript B refers to the bath values and no subscript to the filter values; μ_i^{ex} is the excess chemical potential; ρ_i is the concentration; and Ψ is the Donnan potential. In terms of these quantities, Fig. 4a plots

$$\frac{\rho_i}{\rho_{\mathrm{B},i}}\exp\left(\frac{ez_i}{kT}\Psi\right) = \exp\left(\frac{\mu_{\mathrm{B},i}^{\mathrm{ex}} - \mu_i^{\mathrm{ex}}}{kT}\right). \quad (3.2)$$

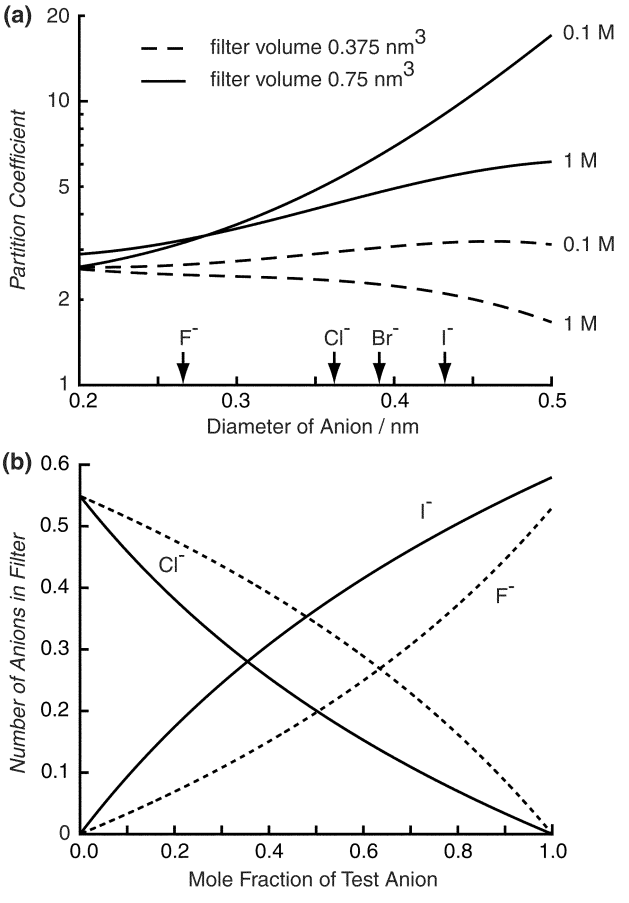

Fig. 4 Selectivities in anion channels. The filters are as described in Fig. 3. (a) The bath contains 0.1 M or 1 M of Na^+ and a monovalent anion whose diameter is varied. (b) The bath contains a mixture of NaCl and either NaF (dotted lines) or NaI (solid lines). The mole fractions of the two salts is varied while the total salt concentration is fixed. The filter volume is 0.75 nm^3.

The Donnan potential has identical effects on anions of the same valence present in mixed electrolyte solutions (for example, in a mole fraction experiment). In that case, the partitioning of both anion species is determined solely by the local excess chemical potentials.[17]

Fig. 4a shows that the small filter is mildly selective for large anions at physiological bath concentrations (100 mM), but switches to preferring small anions at elevated bath concentrations (1 M). The large filter, on the other hand, always prefers larger anions. This difference reflects the different extents of crowding: the small filter tends to be crowded by anions seeking to neutralize the structural charge, whereas the large filter is not. Fig. 4b shows the results of two direct competition (mole fraction) experiments for the larger filter, one with NaF/NaCl mixtures and one with NaI/NaCl mixtures.

C Variable filter volume

It is clear that the filter dimensions play a key role in selectivity phenomena. Indeed, in the view of selectivity given here, the main role of the channel protein is to provide the structural charge, an apolar surface, and volume needed to support selectivity. Figs. 1–4 were computed with constant volume, but, as discussed in ref. 7, the filter volume, instead, may vary while the pressure inside the filter is held constant; that is, the channel protein provides a flexible, constant-pressure environment. We explore this simple possibility by fixing the relative pressure at −100 MPa, the pressure at low bath concentrations of the 0.75 nm^3 channel discussed above. Because the filter/bath pressure difference is negative, the filter accumulates ions, and the filter volume increases, as seen in Fig. 5a. However, because the volume cannot increase forever, we also consider the possibility that the channel protein allows the filter to expand at constant pressure up to a maximal volume. For the example, we choose this maximal volume to be 1 nm^3.

Fig. 5b shows the number of ions accumulated in a filter with variable volume. The dotted lines indicate the 0.75 nm^3 fixed-volume case of Fig. 3a. The dashed and solid lines show that the accumulation of ions is amplified in variable volumes; a lower bath concentration in the variable-volume case has the same effect as a larger concentration in the fixed-volume case. Furthermore, once the maximal volume is reached, the filter still accumulates ions, but the concentration dependence is qualitatively different.

D Conductance

The opening of ClC chloride channels is regulated by transmembrane voltage, but the voltage at which the channels open shifts with the extracellular concentration of Cl^-.[15] Cl^- entering the extracellular mouth of the closed channel is thought to force open the pore, thereby acting as a "gating particle" whose movement is driven by the electric field and prepares the passage of other ions through the channel (reviewed in ref. 16). While in these channels Cl^- appears to regulate conductance like a switch, it seems to have a graded effect on conductance in a neuronal background anion channel (NBAC) of yet unknown molecular identity.[19] Here, the conductance seems to vary gradually with Cl^- concentration; it is proportional to bath Cl^- concentration at low salt concentrations, increases hyperlinearly at intermediate salt concentrations, and less steeply beyond.

We associate volume changes like those shown in Fig. 5a with such "regulatory" changes in channel conductance. Ion-related pressure changes in the pore will modify channel cross-section, as allowed by the mechanics of the protein (the stress exerted on the pore wall in our examples is substantial: a pressure of 100 MPa in a cylindrical pore 1 nm in diameter and 1 nm in length produces 314 pN of stress). As a measure of the conductance near equilibrium we use the product of

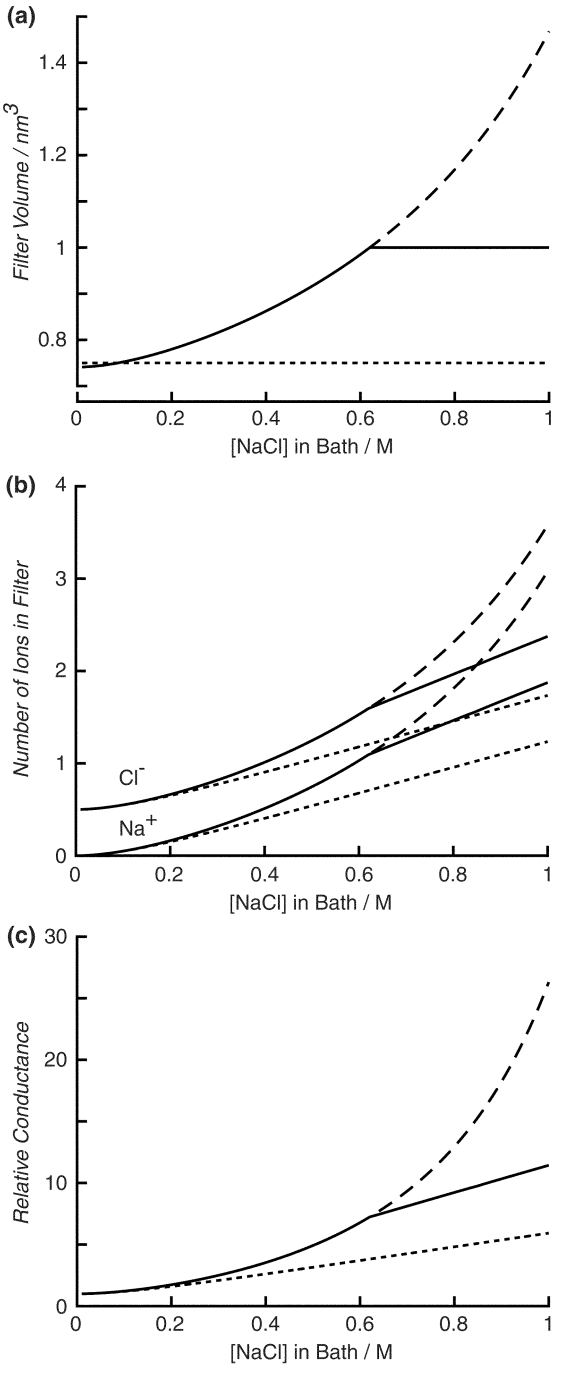

Fig. 5 Effects of mechanical interaction between filter contents and channel protein. Three cases are considered: a rigid protein (dotted lines), a protein that maintains a constant negative pressure in the filter (−100 MPa, dashed lines), and a protein that maintains −100 MPa of filter pressure but limits filter volume to $\leqslant 1$ nm^3 (solid lines). The bath contains a model NaCl electrolyte of varied salt concentration. (a) filter volumes; (b) number of ions in the filter; (c) normalized conductances.

the total number of permeable ions in the channel (Fig. 5b) and the area of the cylindrical filter [ref. 18, eqn. (29.116)]. We assume that the electrophoretic mobilities of all ions are equal and that any change in volume is only in the radial direction,[7] making the cross-sectional area proportional to the filter volume (Fig. 5a). In Fig. 5c we plot this measure of conductance, normalized to the value at 10 mM. The curves for the two variable-volume cases discussed above are approximately linear at low bath concentrations, but then increase hyperlinearly for higher bath concentrations. If the channel is simply allowed to expand, then the conductance increases

hyperlinearly without limit; if the channel can expand only to a maximal volume, however, the conductance increases much less rapidly after increasing hyperlinearly, much as has been observed in NBAC channels.[19]

IV. Cation channels

The large-ion selectivity in our model involves a solvent–channel interaction and excluded volume and therefore similar effects could occur in cation channels. Indeed, gramicidin A (gA) and the nicotinic acetylcholine receptor (nAchR) do show preferences for large cations, albeit to different extents.[1] To model these channels we simplify their structure as we did with the anion channel. In this case, each channel contains two oxygen atoms, each with a charge of $-1/2$ and diameter 0.28 nm. These groups are chosen to attract, on average, one cationic charge to the filter and can be replaced by a more realistic description of the filter charge, if desired. The two differences between the channels are their volumes (0.3 nm^3 for gA and 1.5 nm^3 for nAchR) and the water penalty ($2kT$ for gA and $0.5kT$ for nAchR). The water penalties are chosen to reflect the different situations of water in these channels: gA forces water into a single file of molecules whereas the wider nAchR exposes water in a less extreme way to the pore wall.

Similar to the anion channel, in Fig. 6 we plot the partition coefficient excluding the Donnan potential contribution as a function of cation diameter to show that both of these very different filters preferentially accumulate larger cations. The simplifications of the channel structures we use are dramatic; our intent is not to fit data, but merely to illustrate that a reasonable choice of parameters can qualitatively give the observed selectivity sequences, as well as the different degrees of cation selectivity of these two channels.

V. Concluding remarks

The main result of this paper is that large-ion selectivity in ion channels can arise as a consequence of unfavorable water/channel interactions. We use the simple representation of the channel and bath as two bulk liquids and describe ions as charged, hard spheres and water as uncharged, hard spheres in a background dielectric. It is clear that more appropriate treatments of the geometry and the confined fluid in the channel should be made;[4] structural information needed for such work has recently become available for two anion channels[2] and has been available for some time for gramicidin A.

Dutzler *et al.* proposed that Cl^- selectivity in ClC channels arises from the specific "coordination" of Cl^- by structural charges.[2] In our model such coordination is not important; we find that the excess pressure and ionic chemical potential due to interionic screening are small compared to those from the excluded volume effect. Our computations suggest that the structural charge is primarily important for providing a charge-selective long-range electric field, with the necessary penalty for water entry perhaps provided by the apolar groups found by Dutzler *et al.* to be lining the filter. Size selectivity among anions then arises from excluded-volume effects. These excluded-volume effects involve very small variations in particle density that are likely to be undetectable in crystallographic measurements at currently available resolutions.

Besides describing selectivity, the proposed mechanism may be important in the blocking of channels by organic ions that bind in wider parts of channels, a mechanism first described by Armstrong to explain the block of voltage-dependent K channels by alkylammonium ions.[20] Indeed, the crystallographic structure of a K channel reveals a wide central cavity that is accessible to molecular ions.[21] This cavity is connected to the intracellular mouth of the channel by a pore whose effective diameter is approximately 0.9 nm.[22] On the other side, it is connected to the narrow selectivity filter which prevents the large ions from moving through the channel to the extracellular side. The cavity is lined by apolar amino acid residues and thus is likely to support the kind of large-particle affinity described here.

Beyond ion channels, the proposed mechanism of large-particle affinity might be generally important in the binding of ligands to partially apolar binding pockets on proteins, as well as in protein–protein interactions.

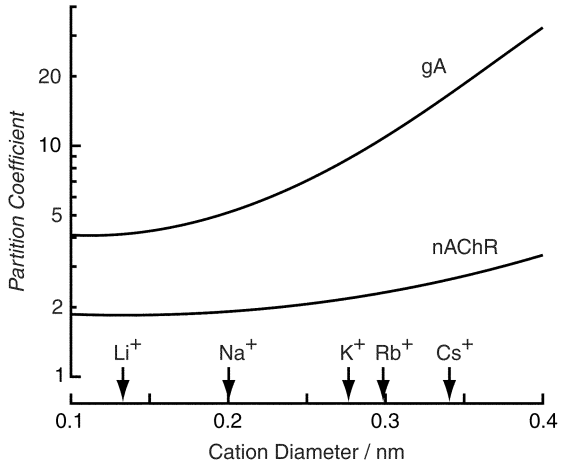

Fig. 6 Cation partition coefficients excluding the Donnan potential in two channels modeling gramicidin A (gA) and the nicotinic acetylcholine receptor (nAChR). The channels confine 2 groups of charge $-1/2$ and diameter 0.28 nm in volumes of 0.3 nm^3 for gA or 1.5 nm^3 for nAChR.

Appendix A: Equilibrating the two compartments

In order that the paper is self-contained we include an outline of the thermodynamics of the bath/filter equilibration. This has previously been published in ref. 7.

To equilibrate the two compartments at constant volume or constant pressure (the two cases we consider), it necessarily follows that the total chemical potentials in boths compartments are equal:

$$\begin{aligned}\mu_i &= \mu_i^0 + \mu_i^{\mathrm{ex}} + kT\,\ln(\rho_i) + e_0 z_i \Psi \\ &= \mu_{\mathrm{B},i} = \mu_{\mathrm{B},i}^0 + \mu_{\mathrm{B},i}^{\mathrm{ex}} + kT\ln(\rho_{\mathrm{B},i}) \qquad \text{(A.1)}\end{aligned}$$

where variables with (first) subscript "B" apply to the bath, variables not subscripted to the filter, and i refers the species. μ is the total chemical potential, μ^0 the standard chemical potential, μ^{ex} the excess chemical potential, ρ the number density, z the valence, Ψ the electrical potential of the filter relative to the bath (Donnan potential), T the temperature, k the Boltzmann constant, and e_0 the elementary charge. For the cases we consider, this equation must be solved subject to the constraint that either the volume V is constant or V is such that the computed pressure P is the pressure P_{prot} exerted by the protein:

$$P(V) = P_{\mathrm{prot}}.$$

We computed the excess thermodynamic properties with the MSA (mean spherical approximation) theory of bulk electrolytes,[11,12,23–28] in which ions are described as charged hard spheres.

For the bath solution, we compute ionic excess chemical potentials with respect to the infinitely dilute solution in water, using the primitive model MSA description of bulk electrolytes developed by Simonin *et al.*[27,28] The standard and excess

chemical potentials of water in the bath are set to zero. In the filter we use the SPM/MSA model of electrolyte solutions, where the solvent is assigned the hard-sphere diameter of water. The dielectric coefficient was assigned a fixed value throughout the system and thus the standard chemical potential differences for all species is zero: $\mu_i^0 - \mu_{B,i}^0 = 0$.

In the filter solution, the excess chemical potential of a species i (ion or water) is expressed in the components

$$\mu_i^{ex} = \mu_i^{ES} + \mu_i^{HS}. \tag{A.2}$$

The electrostatic (ES) component is described by

$$\mu_i^{ES} = -\frac{e_0^2}{4\pi\varepsilon\varepsilon_0}\left[\frac{\Gamma z_i^2}{1+\Gamma\sigma_i} + \eta\sigma_i\left(\frac{2z_i - \eta\sigma_i^2}{1+\Gamma\sigma_i} + \frac{\eta\sigma_i^2}{3}\right)\right]. \tag{A.3}$$

where ε_0 is the permittivity of vacuum. The MSA screening parameter Γ is given by the implicit relation

$$4\Gamma^2 = \frac{e_0^2}{kT\varepsilon\varepsilon_0}\sum_i \rho_i\left[\frac{z_i - \eta\sigma_i^2}{1+\Gamma\sigma_i}\right]^2 \tag{A.4}$$

and the MSA parameter η represents the effects of non-uniform molecular diameters σ_i:

$$\eta = \frac{1}{\Omega}\frac{\pi}{2\Delta}\sum_j \frac{\rho_j\sigma_j z_j}{1+\Gamma\sigma_j} \tag{A.5}$$

$$\Omega = 1 + \frac{\pi}{2\Delta}\sum_j \frac{\rho_j\sigma_j^3}{1+\Gamma\sigma_j} \tag{A.6}$$

where Δ is defined below. The electrostatic interactions contribute the (negative) excess pressure

$$P^{ES} = -\frac{\Gamma^3}{3\pi} - \frac{e_0^2\eta^2}{2\pi^2 kT\varepsilon\varepsilon_0}. \tag{A.7}$$

The hard-sphere (HS) component of the excess chemical potential, expressed relative to the pure filter solvent, is

$$\mu_i^{HS} = \mu_{act,i}^{HS} - \mu_{ref,i}^{HS} \tag{A.8}$$

where the terms on the right-hand side are computed from the expressions[29,30]

$$\frac{\mu_{x,i}^{HS}}{kT} = -\ln(\Delta) + \frac{3\xi_2\sigma_i + 3\xi_1\sigma_i^2}{\Delta} + \frac{9\xi_2^2\sigma_i^2}{2\Delta^2} + \frac{\pi P_x^{HS}\sigma_i^3}{6kT} \tag{A.9}$$

$$\frac{\pi P_x^{HS}}{6kT} = \frac{\xi_0}{\Delta} + \frac{3\xi_1\xi_2}{\Delta^2} + \frac{3\xi_2^3}{\Delta^3} \tag{A.10}$$

$$\xi_n = \frac{\pi}{6}\sum_j \rho_{x,j}\sigma_j^n \tag{A.11}$$

$$\Delta = 1 - \xi_3. \tag{A.12}$$

This is derived *via* the compressibility route. For the ions, the actual densities (subscript "act") are the densities in the filter solution and the reference densities (subscript "ref") are zero (infinitely dilute solution of the ion species in filter solvent). For the solvent (neutral hard spheres with the diameter of water) the actual density is that of the solvent present in the filter and the reference density is that of pure water. The subtraction in eqn. (1.8) establishes (at infinite dilution) the filter solvent as the reference for excess chemical potentials in the filter. Similarly, the (excess plus ideal) pressure in the hard-sphere liquid of the filter is computed from

$$P^{HS} = P_{act}^{HS} - P_{ref}^{HS}. \tag{A.13}$$

Solvent and ionic diameters used to model the filter solution are listed in the main text and figure legends.

Acknowledgements

This work was supported by grants from NIH (T32NS07044 to D. G.), NSF (CHE98-13729 to D. H.), and DARPA (W. N. and R. S. E.).

References

1 B. Hille, *Ion Channels of Excitable Membranes*, Sinauer Associates, Inc., Sunderland, MA, 3rd edn., 2001.
2 R. Dutzler, E. B. Campbell, M. Cadene, B. T. Chait and R. Mackinnon, *Nature*, 2002, **415**, 287–294.
3 D. Goulding, J.-P. Hansen and S. Melchionna, *Phys. Rev. Lett.*, 2000, **85**, 1132–1135.
4 D. Goulding, S. Melchionna and J.-P. Hansen, *Phys. Chem. Chem. Phys.*, 2001, **3**, 1644–1654.
5 G. K. Percus and G. J. Yevick, *Phys. Rev.*, 1958, **110**, 1.
6 W. Nonner, L. Catacuzzeno and B. Eisenberg, *Biophys. J.*, 2000, **79**, 1976–1992.
7 W. Nonner, D. Gillespie, D. Henderson and B. Eisenberg, *J. Phys. Chem. B*, 2001, **105**, 6427–6436.
8 D. Gillespie, W. Nonner and R. S. Eisenberg, *J. Phys.: Condens. Matter*, 2002, in press.
9 E. Spohr, A. Trokhymchuk and D. Henderson, *J. Electroanal. Chem.*, 1998, **450**, 281–287.
10 E. Waisman and J. L. Lebowitz, *J. Chem. Phys.*, 1970, **52**, 4307.
11 E. Waisman and J. L. Lebowitz, *J. Chem. Phys.*, 1972, **56**, 3093.
12 L. Blum, *Mol. Phys.*, 1975, **30**, 1529.
13 S. S. Smith, E. D. Steinle, M. E. Meyerhoff and D. C. Dawson, *J. Gen. Physiol.*, 1999, **114**, 799–817.
14 F. Franciolini and W. Nonner, *J. Gen. Physiol.*, 1994, **104**, 711–724.
15 M. L. Pusch, U. Ludewig, A. Rehfeldt and T. J. Jentsch, *Nature*, 1995, **373**, 527–531.
16 M. Maduke, C. Miller and J. A. Mindell, *Annu. Rev. Biophys. Biomol. Struct.*, 2000, **29**, 411–438.
17 D. Gillespie and R. S. Eisenberg, *Eur. Biophys. J.*, 2002, **31** (DOI: 10.1007/s00249-002-0239-x).
18 R. S. Berry, S. A. Rice, J. Ross, *Physical Chemistry*, 2000, Oxford University Press, New York.
19 F. Franciolini and W. Nonner, *J. Gen. Physiol.*, 1994, **104**, 725–746.
20 C. M. Armstrong and L. Binstock, *J. Gen. Physiol.*, 1965, **48**, 859–872.
21 D. A. Doyle, J. M. Cabral, R. A. Pfuetzner, A. Kuo, J. M. Gulbis, S. L. Cohen, B. T. Chait and R. MacKinnon, *Science*, 1998, **280**, 69–77.
22 C. M. Armstrong, *Q. Rev. Biophys.*, 1975, **7**, 179–210.
23 R. Triolo, J. R. Grigera and L. Blum, *J. Phys. Chem.*, 1976, **80**, 1858.
24 R. Triolo, L. Blum and M. A. Floriano, *J. Phys. Chem.*, 1978, **82**, 1368.
25 R. Triolo, L. Blum and M. A. Floriano, *J. Chem. Phys.*, 1978, **67**, 5956.
26 L. Blum and J. S. Høye, *J. Phys. Chem.*, 1977, **81**, 1311.
27 J.-P. Simonin, L. Blum and P. Turq, *J. Phys. Chem. B*, 1996, **100**, 7704.
28 J.-P. Simonin, *J. Phys. Chem. B*, 1997, **101**, 4313.
29 J. L. Lebowitz, *Phys. Rev., Sect. A*, 1964, **133**, 895.
30 J. J. Salacuse and G. Stell, *J. Chem. Phys.*, 1982, **77**, 3714.